Finite Chain Extensibility and Topological Constraints in Swollen Networks

M. Klüppel*

Deutsches Institut für Kautschuktechnologie e.V., Hannover, Germany

Received September 27, 1993; Revised Manuscript Received February 28, 1994®

ABSTRACT: Uniaxial stress–strain properties of highly swollen and stretched rubbers are discussed in the framework of a recently developed non-Gaussian network model that considers the finite extensibility of network chains together with topological chain constraints. The finite extensibility is described by the well-known inverse Langevin function of the network chain end-to-end distance. The model consequently distinguishes between topological constraints coming from packing effects of neighboring chains and from trapped entanglements. Whereas the latter act as additional network junctions, the packing effects are modeled in a mean-field-like manner through strain-dependent conformational tubes. The calculated Gaussian contribution to the total modulus, the swelling dependence of the infinite strain modulus, and the tube constraint modulus of natural rubber (NR) samples are determined. It is found that the infinite strain modulus varies linearly with the polymer volume fraction ϕ, whereas the tube constraint modulus varies as $\phi^{4/3}$. Both observations agree with the predictions of the presented model. Contrary to literature data that were estimated from stress–strain experiments on swollen networks in the framework of Gaussian statistics, the tube constraint modulus (which is proportional to the C_2 value of the Mooney–Rivlin equation) is found to vanish in the limit $\phi \to 0$, and not at a finite universal value $\phi \approx 0.2$.

1. Introduction

A comprehensive theory of elasticity must account for the swelling dependence of the stress–strain properties of swollen polymer networks. Several pioneering experimental investigations of Mullins et al.[1,2] led to the following features that are reviewed in ref 3: (i) The phenomenological Mooney–Rivlin constant C_1 is essentially independent of swelling, whereas C_2 decreases significantly with decreasing volume fraction ϕ of the polymer in the swollen network. (ii) In particular, the empirical relation $C_2(\phi) = C_2(\phi=1)\phi^k$ with $^1/_3 \le k \le {}^4/_3$ may be quoted.[3] In addition, it is known that C_2 in general becomes zero at $\phi \approx 0.2$, independent of polymer type and swelling agent.

A qualitative molecular explanation of these properties is possible on the basis of the model of restricted junction fluctuations[4–6] and of various tube models of rubber elasticity that relate the C_2 term of the Mooney–Rivlin equation to topological constraints acting on the network chains.[7–11] These tube models assume that, due to the high coil interpenetration in dry rubbers, the cross-links and chain segments are not allowed to fluctuate freely but are forced to remain in a virtual conformational tube that is built by the surrounding chains. Upon swelling, the coil interpenetration is reduced and the tube diameter increases, resulting in a reduction of the topological constraint contribution to the retracting force, i.e., a decrease of the C_2 term.

A quantitative theory of tubelike topological constraints was derived self-consistently by Heinrich et al.[7,12] The estimate of the lateral tube diameter d_0 from stress–strain data leads in all cases of investigated unswollen rubbers to the relation $l_s < d_0 < R_c$, where l_s is the statistical segment length and $R_c \sim \mu^{-1/2}$ is the average end-to-end distance of network chains.[13,14] The chemical cross-link density μ determined by the tube concept from stress–strain data was proved by Gronski et al. to be in agreement with corresponding ^{1}H- and ^{13}C-NMR results.[15] The estimated value of the tube diameter d_0 was proved to be in agreement with direct neutron scattering results.[16] The tube model predicts an asymptotic decrease of topological constraints with swelling and a total disappearance in the limit of an infinite dilution of the network. However, as already mentioned above, the experimental results suggest a vanishing influence of topological constraints at a finite degree of swelling. For this reason, a fitting parameter β ($0 \le \beta \le 1$) was introduced into the tube model that was assumed to be related to different constraint release effects of network chains.[7] A value $\beta < 1$ was assumed to reflect the influence of network imperfections and/or swelling agent on mechanical properties. Later on, the parameter β was used to explain discrepancies between neutron scattering experiments and calculated scattering functions.[7,17] However, the physical significance of constraint release effects still remains unproved.

The tube model and the semiempirical Mooney–Rivlin equation are founded on Gaussian chain statistics that does not take into account the finite extensibility of network chains. Hence, in a strict sense, these models can be applied in the limit of small deformations only. Any extrapolation to larger deformations, as is done in the Mooney–Rivlin plots, should be performed carefully. It was shown by different authors that systematic deviations between Gaussian and non-Gaussian statistics occur not only in the "upturn range" at large extensions but also for small and medium deformations.[2,18–22] In previous papers it was demonstrated that the C_2 term is generally larger if inverse Langevin statistics is applied instead of Gaussian statistics.[20–22] Therefore, it is expected that the limiting polymer volume fraction that is related to vanishing topological constraints is smaller than $\phi \approx 0.2$ if inverse Langevin statistics is used instead of Gaussian statistics. We will show that the consideration of constraint release effects of network chains is not necessary for understanding the swelling dependence of the topological constraint modulus if a generalized model is applied that is related to an inverse Langevin approximation for the distribution of chains. Throughout this paper we assume no constraint release effects and hence we take $\beta = 1$ without restrictions of generality.[12]

The paper is organized as follows: In section 2 the tube model is applied to stretched and swollen networks. A

* Present address: Dr. Manfred Klüppel, Am Tongrund 1, 30974 Wennigsen, Germany.

® Abstract published in *Advance ACS Abstracts*, May 1, 1994.

0024-9297/94/2227-7179$04.50/0

generalization takes into account the finite extensibility of network chains. Sections 3 and 4 offer experimental investigations of uniaxial stress–strain properties of swollen natural rubber samples with varying cross-linking density and swelling agent. Section 5 contains some conclusions concerning the competitiveness and power of the tube model of swollen rubbers.

2. Theory

The various theories of tubelike topological constraints in polymer networks explain the deviations from classical network models (e.g., the C_2 term of the Mooney–Rivlin equation) by an anisotropic deformation of the tubes that leads to an additional contribution to the elastic free energy of the network.[7] In general, the following deformation law for the lateral tube dimension is assumed:

$$r_i = r_0\lambda_i^{\nu} \qquad i = 1,2,3 \tag{1}$$

where r_0 is the tube radius in the undeformed state and λ_i is the deformation ratio in direction i of the principal axis of the deformation tensor. The exponent ν describes different constraint mechanisms and varies between $\nu = -1$ and $\nu = 1$ in the various models.[7-12,23] An affine deformation of the tubes ($\nu = 1$) was first discussed by Edwards,[23] while other authors proposed deformation laws that follow from the assumption of constant tube volume or special entanglement models.[8-11] The theory of Heinrich et al. leads to the nonaffine prediction $\nu = 1/2$ for moderately cross-linked rubbers as well as for un-cross-linked, entangled melts where the number of constraining chains acting on a test chain is large.[7,12] The case of moderately cross-linked networks is characterized by a large degree of coil interpenetration of network chains and, therefore, a large so-called Flory number $N_F = (n_s l_s^3)N^{1/2} \gg 1$. Here, n_s denotes the number of chain segments per unit volume, l_s is the statistical segment length, and N is the number of segments between two connected covalent cross-links.

Throughout this paper we will assume the value $\nu = 1/2$ for the deformation exponent that is relevant for the investigated moderately cross-linked rubber samples. We will first evaluate the stress–strain behavior of swollen rubbers in the low-strain limit, i.e., in the framework of Gaussian statistics. In a second step we will generalize the results to non-Gaussian statistics, which allows an application to large deformations.

2.1. Gaussian Networks. As discussed in previous papers,[20-22] the elastic free energy density of a deformed network can be calculated by assuming three different influences on a single network strand between two chemical cross-links: The first one results from the two chemical cross-links of the strand. The second influence arises from trapped entanglements of the strand under consideration that act like additional junctions. The third influence results from the suppression of segment fluctuation by the surrounding chains (packing effects) and is taken into account by the constraining potential of a tube model.[7,12] All three influences are assumed to be decoupled and additive.[24] The free energy density of a first swollen and then stretched Gaussian network is given by

$$\Delta W_{el}(\phi,\lambda_i) = (G_c(\phi) + G_e(\phi)T_e)\, I_1(2,1) - 2G_N(\phi)\, I_1(-1,1) \tag{2}$$

where $I_1(x,y)$ is a generalized deformation invariant:[7]

$$I_1(x,y) = \frac{\sum_{i=1}^{3}(\lambda_i\lambda_{i,sw})^{xy} - 3}{xy} \tag{3}$$

$\lambda_{i,sw}$ is the deformation ratio in spatial direction i and is determined by the degree of swelling. The quantity λ_i denotes the deformation ratio in spatial direction i and results from the stretching after swelling. λ_i is related to the dimensions of the swollen samples, and hence, the product $\lambda_i\lambda_{i,sw}$ equals the total deformation ratio in spatial direction i. T_e is the trapping factor of interchain entanglements, and $G_c(\phi)$, $G_e(\phi)$, and $G_N(\phi)$ are swelling-dependent moduli that correspond to cross-links, entanglements, and tubelike topological constraints, respectively. In terms of molecular quantities the moduli are given by the following expressions:[20-22,25]

$$G_c(\phi) = A_c\nu_c(\phi)RT = \frac{A_c\hat{\rho}_p(\phi)l_s^2RT}{M_sR_c^2} \tag{4}$$

$$G_e(\phi) = A_e\nu_e(\phi)RT = \frac{A_e\hat{\rho}_p(\phi)l_s^2RT}{M_sR_e^2} \tag{5}$$

$$G_N = \frac{\hat{\rho}_p(\phi)l_s^2RT}{4\sqrt{6}M_sr_0^2(\phi)} \tag{6}$$

A_c and A_e are microstructure factors that depend on the degree of fluctuations of cross-links and entanglements, respectively.[24] R is the gas law constant, T is the absolute temperature, M_s is the molar mass, and l_s is the length of the statistical segments. R_c and R_e are the mean distances of successive cross-links and entanglements in the undeformed state, respectively. $\nu_c(\phi)$ and $\nu_e(\phi)$ denote the swelling-dependent molar number densities of elastically effective network strands related to cross-links and entanglements. $\hat{\rho}_p(\phi)$ is the swelling-dependent mass density of the elastically effective network and is related to the mass density $\rho_p(\phi)$ of the whole sample (including sol molecules and chain ends) via the trapping factor T_e and the gel fraction w_g:[26-28]

$$\hat{\rho}_p(\phi) = \left(\frac{3}{2}T_e^{1/2}w_g - \frac{T_e}{2}\right)\rho_p(\phi) \tag{7}$$

The swelling dependence of the mass density $\hat{\rho}_p$ as well as the molar number densities ν_c and ν_e is given by

$$\hat{\rho}_p(\phi) = \phi\hat{\rho}_p(\phi=1) \tag{8}$$

$$\nu_c(\phi) = \phi\nu_c(\phi=1) \tag{9}$$

$$\nu_e(\phi) = \phi\nu_e(\phi=1) \tag{10}$$

The swelling dependence of the tube radius $r_0(\phi)$ follows directly from the tube deformation law eq 1 with $\nu = 1/2$, because swelling corresponds to a triaxial stretching of the sample with

$$\lambda_{i,sw} = \phi^{-1/3} \qquad i = 1,2,3 \tag{11}$$

Hence, we conclude from eq 1

$$r_0(\phi) = \phi^{-1/6}r_0(\phi=1) \tag{12}$$

Then, we find for the moduli (4)–(6)

$$G_c(\phi) = \phi\, G_c(\phi=1) \tag{13}$$

$$G_e(\phi) = \phi\, G_e(\phi=1) \tag{14}$$

$$G_N(\phi) = \phi^{4/3} G_N(\phi=1) \tag{15}$$

The dependence of the retracting force $f(\phi)$ on the polymer volume fraction in a uniaxially stretched and swollen network is evaluated by choosing $\lambda = \lambda_1$ in the direction of strain and assuming the incompressibility condition:

$$\lambda_1\lambda_2\lambda_3 = 1 \tag{16}$$

The mechanical stress $\sigma(\phi) = f(\phi)/Q_0(\phi)$ in the direction of strain results from eqs 2, 3, and 11:

$$\sigma(\phi) = \frac{d}{d\lambda}(\Delta W_{el}(\phi,\lambda)) = \left[(G_c(\phi) + G_e(\phi)T_e)\phi^{-2/3} + G_N(\phi)\phi^{1/3}\frac{2(\lambda^{1/2} - \lambda^{-1})}{\lambda^2 - \lambda^{-1}}\right](\lambda - \lambda^{-2}) \tag{17}$$

The stretching force $f(\phi)$ is usually related to the cross section $Q_0(\phi)$ of the swollen sample before uniaxial deformations. This cross section can also be expressed by the cross section Q_0 of the undeformed, unswollen sample by using the relation

$$Q_0(\phi) = Q_0\phi^{-2/3} \tag{18}$$

Hence, the reduced (or Mooney) stress, which is related to the cross section Q_0 of the unswollen sample and the extension ratio λ relative to the swollen sample, is given by

$$\sigma_{red}(\phi) = \frac{f(\phi)}{Q_0(\lambda - \lambda^{-2})} \tag{19}$$

We finally find in the framework of Gaussian statistics

$$\sigma_{red}(\phi) = (G_c(\phi=1) + G_e(\phi=1)T_e)\phi^{-1/3} + G_N(\phi=1)\,\phi\frac{2(\lambda^{1/2} - \lambda^{-1})}{\lambda^2 - \lambda^{-1}} \approx (G_c(\phi=1) + G_e(\phi=1)T_e)\phi^{-1/3} + G_N(\phi=1)\phi\lambda^{-1} \quad \text{for } \lambda \geq 1 \tag{20}$$

From eq 20 it follows that a Mooney–Rivlin plot of the product $\sigma_{red}\phi^{1/3}$ against λ^{-1} should result in a linear dependence. The axis intersection of this function, extrapolated at infinite strain, is expected to be independent of ϕ and the slope should vary as $\phi^{4/3}$. This prediction can be tested experimentally by performing uniaxial stress–strain measurements on differently swollen networks. It allows a direct examination of the deformation law (1) and, hence, the assumed value $\nu = {}^1/_2$ for the exponent.

2.2. Non-Gaussian Approximations. For an application up to large extensions, eq 20 has to be generalized to non-Gaussian statistics that takes into account the finite extensibility of the network chains. This is done by considering the conformational entropy contribution resulting from the orientation of chain segments. It leads to an expression for the end-to-end distribution of network chains that involves the inverse Langevin function instead of the Gaussian distribution function. By using a series expansion for the inverse Langevin function, the first two terms of eq 20 can be easily modified.[19] The third term, which results from tubelike topological constraints, is much more difficult to deal with, because the tube model (and hence its consequences like eq 1 and the modulus G_N) are founded on the assumption of Gaussian network chains. However, recent molecular-statistical investigations of tubelike network models based on non-Gaussian network chains clearly showed that the action of tube constraints becomes weaker in the case of a predominance of finite chain extensibility.[29–31] Heinrich and Beckert quantified this conclusion using a wormlike chain model in spherical approximation.[29] They calculated the free energy change of tubelike constrained chains where the tubes themselves are self-consistently built from the finite wormlike chains.[29] Similar results were obtained by Edwards and Vilgis using a renormalized Gaussian chain model with diverging entropy in the fully stretched state[30] and by Kovac and Crabb using a modified Gaussian three-hard-tube model of rubber elasticity.[31] To summarize these findings, we may assume that the influence of finite extensibility on the third term of eq 20 is expected to be small in the case of large deformations. Hence, it seems reasonable to approximate the tubelike topological constraints in the framework of Gaussian statistics only. Then instead of eq 20, we find the more general expression[21,22]

$$\sigma_{red}(\phi) \approx (G_c(\phi=1) + G_e(\phi=1)T_e)\phi^{-1/3}\left\{1 + \frac{3}{25n}\left(3\lambda^2 + \frac{4}{\lambda}\right) + \frac{297}{6125n^2}\left(5\lambda^4 + 8\lambda + \frac{8}{\lambda^2}\right) + \ldots\right\} + G_N(\phi=1)\,\phi\lambda^{-1} \tag{21}$$

n is the average number of statistical segments between successive junctions that are built by cross-links as well as trapped entanglements:

$$n = \frac{\hat{\rho}_p(\phi=1)}{(\nu_c(\phi=1) + \nu_e(\phi=1)T_e)M_s} = \frac{\hat{\rho}_p(\phi=1)RT}{\left(\frac{G_c(\phi=1)}{A_c} + \frac{5}{4}G_N^{\circ}T_e\right)M_s} \tag{22}$$

In the second part of eq 22 a relation between $\nu_e(\phi=1)$ and the plateau modulus G_N° of the un-cross-linked polymer melt is used.[21,22] Obviously, the segment number n is independent of ϕ, which means that it can be determined by measurements of unswollen networks alone. The iterative way for the evaluation of this number is demonstrated in detail in refs 21 and 22.

The segment number n determines the limiting extensibility of the network chains by the relation $\lambda_{max} = n^{1/2}$, where the full series expansion of eq 21 approaches infinity. In the limit $n \to \infty$, a Gaussian statistics, i.e., eq 20, results. It is seen that only the first term of the series expansion in eq 21 describes the Gaussian contribution to the reduced stress. This contribution can be evaluated from eq 21 if the segment number n is known. Following this way, it is possible to test the validity of the Gaussian network model, presented in section 2.1, by comparing the experimentally observed uniaxial stress–strain properties of unswollen and swollen networks.

3. Materials and Experimental Procedures

Natural rubber samples (SMR-CV50) were cured at 155 °C with varying concentrations of the cross-linking agent tetramethylthiuram disulfide (TMTD) together with the same amount of ZnO. The cross-linking procedure was performed almost completely up to 90% of the maximum torque found in vulcameter measurements. From the cured rubber sheets, strip samples were stamped out for measuring the uniaxial stress–strain properties.

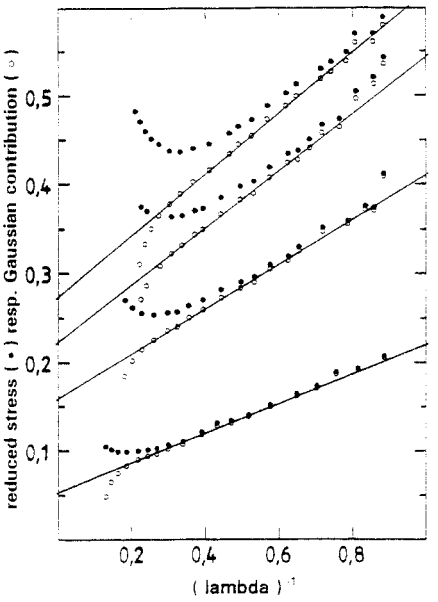

Figure 1. Mooney–Rivlin plot at 373 K (●) and the calculated Gaussian contribution (○) for NR networks cured with 1, 2, 3, and 4 phr TMTD.

Table 1. List of Swelling Diluents Together with Their Boiling Temperatures

diluent	boiling temp/°C	diluent	boiling temp/°C
1-propanol	98	cyclopentanone	131
1-hexanol	158	cyclohexanone	156
1-heptanol	176	chlorobenzene	133
1-octanol	195	bis(2-ethylhexyl) phthalate	386
1-decanol	232	bis(2-ethylhexyl) sebacate	172

Part of the samples were swollen up to equilibrium in different diluents. They are listed in Table 1 together with their boiling points. The equilibrium swelling degree was measured gravimetrically using separate cylindrical probes.

The uniaxial stress–strain properties of the unswollen and swollen samples were determined by using an optical system for the strain measurements (Universalprüfmaschine Zwick 1445) and applying low extension rates (10 mm/min). The unswollen samples were measured at room temperature (297 K) and at 373 K for evaluating the influence of stress-induced crystallization. The swollen samples were measured at room temperature only. For detecting the stress–strain properties of the swollen samples, it was necessary to take the swollen strip probes out of the diluent. This means that it was not possible to perform the measurements under equilibrium swelling conditions, and consequently, deswelling effects occurred during the stress–strain measurements. The extent of deswelling during the measurements was estimated by weighing the samples before and after the measurement. Apart from extremely highly swollen samples, deswelling effects were found to be negligible. Hence, they are not taken into account in the following.

4. Results and Discussion

Figure 1 shows the Mooney–Rivlin plots of measured stress–strain curves at 373 K for four different unswollen samples that were cured with varying amounts of cross-linking agent (TMTD). In addition, the Gaussian contributions to the reduced stress (eq 20) are shown. They are calculated according to eqs 21 and 22 by assuming $\phi = 1$ and taking the series expansion up to fourth order in n, which yields a good approximation of the inverse Langevin function up to $\lambda/n^{1/2} \approx 0.7$ (compare ref 19 for the expansion coefficients up to fourth order). The parameter n is estimated by using an iteration procedure that determines the moduli $G_c(\phi=1)$ and $G_e(\phi=1)$ and the trapping factor T_e as well as $\hat{\rho}_p(\phi=1)$. The procedure is described in detail in refs 21 and 22. The molar mass of the statistical segments is taken from refs 32 and 33 to be $M_s = 130$ g/mol. The microstructure factor A_c is calculated in the framework of the theory of restricted junction fluctuations,[24] which yields the value $A_c = 0.67$ (compare also ref 25). The plateau modulus of the melt was measured under dynamical shearing conditions as $G_N^\circ = 0.54$ N/mm² at 373 K and $G_N^\circ = 0.45$ N/mm² at 297 K. The gel fraction was approximated as $w_g = 1$.

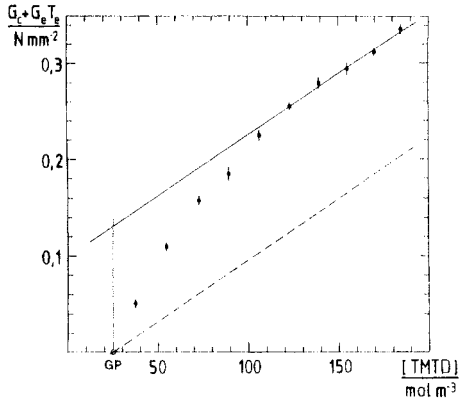

Figure 2. Plot of the infinite strain modulus $G_1 = G_c + G_eT_e$ at 373 K vs concentration of cross-linking agent TMTD. (GP, gel point; (– – –), cross-link contribution G_c.)

The regression lines inserted in Figure 1 are related to the observed linear behavior of the Gaussian contribution to the reduced stress on a large deformation scale. The deviations from the regression lines at large extensions are probably due to a bursting of single chains, while the deviations at small extensions may be related to an insufficient calibration between the zero of stress and strain, which is difficult to realize if the measurements are performed at a large deformation scale. The regression lines determine the infinite strain moduli $G_c + G_eT_e$ and the topological constraint moduli G_N for the four differently cross-linked samples according to eq 20 with $\phi = 1$. It is found that the infinite strain modulus and the topological constraint modulus increase with increasing concentration of cross-linking agent. Figure 2 shows the infinite strain modulus, found from the axis intersections at infinite strain, plotted against the concentration of cross-linking agent TMTD. Starting from a gel point (GP), in the lower concentration regime a nonlinear dependence is observed. However, for TMTD concentrations larger than about 120 mol/m³, an almost linear dependence results. An extrapolation of the corresponding regression line to the concentration of cross-linking agent at the gel point (GP) gives a nonzero contribution to the infinite strain modulus. As G_c is assumed to vanish at the gel point, this contribution corresponds to the limiting amount of trapping ($T_e = 1$) that is reached at about 120 mol/m³ TMTD. The results of Figure 2 confirm the assumed additive structure of the infinite strain modulus, as stated in eq 2.

The results of stress–strain measurements that were performed on the unswollen samples at room temperature (297 K) are summarized in Table 2. Besides the concentration of cross-linking agent (TMTD), the infinite strain moduli $G_c + G_eT_e$, the topological constraint moduli G_N as well as the cross-link contribution G_c to the total modulus, the mass density of elastically effective chains $\hat{\rho}_p$, and the trapping factor T_e are shown. All values are estimated by using the iteration procedure founded on eqs 21 and 22 for $\phi = 1$. The procedure was developed in previous papers.[21,22] The results listed in Table 2 correlate well with the results at 373 K that are shown in Figures 1 and 2 if the temperature dependence of the moduli is

Table 2. List of Network Parameters for Five Differently Cured NR Samples[a]

sample type	[TMTD]/ phr[b]	G_I/MPa	G_N/MPa	G_c/MPa	$\hat{e}_p$/ (kg m^{-3})	T_e
A	1.5	0.10	0.18	0.04	801	0.6
B	2.5	0.16	0.25	0.07	885	0.83
C	3.5	0.22	0.27	0.11	930	1
D	4.5	0.25	0.285	0.14	930	1
E	5.5	0.28	0.30	0.17	930	1

[a] The parameters are found from stress–strain measurements of the unswollen samples at 297 K (room temperature). $G_I = G_c + G_eT_e$, infinite strain modulus; G_c, cross-link contribution to the infinite strain modulus; G_N, topological constraint modulus; T_e, trapping factor; $\hat{e}_p$, mass density of elastically effective chains. The determination procedure for these parameters is demonstrated in detail in refs 21 and 22. [b] phr = per hundred rubber.

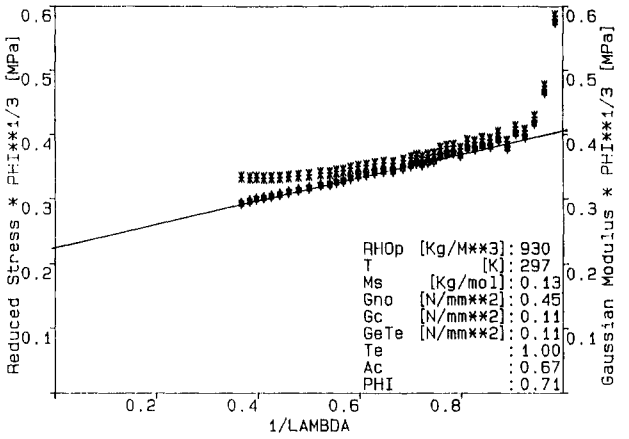

Figure 3. Mooney–Rivlin plot at 297 K, showing the generalized reduced stress $\sigma_{red}\phi^{1/3}$ and its calculated Gaussian contribution of a sample of type C that is swollen in 1-decanol up to equilibrium at $\phi = 0.71$.

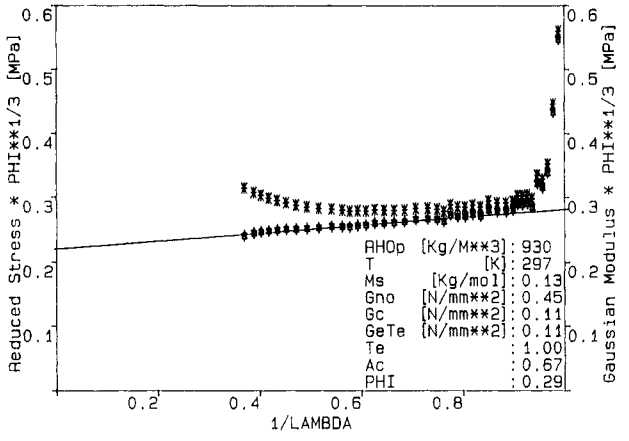

Figure 4. Mooney–Rivlin plot at 297 K, showing the generalized reduced stress $\sigma_{red}\phi^{1/3}$ and its calculated Gaussian contribution of a sample of type C that is swollen in cyclohexanone up to equilibrium at $\phi = 0.29$.

taken into account. This means that the influence of stress-induced crystallization on the determination of the above moduli can be neglected. It is shown elsewhere that a significant difference for the Gaussian contributions to the reduced stress at low and high temperature occurs at very large extensions only, which are not considered for the construction of the regression lines.[34]

Figures 3 and 4 show examples of modified Mooney–Rivlin plots at room temperature (297 K) for two differently swollen samples of the same type C (Table 2). The equilibrium swelling degrees of the samples correspond to polymer volume fractions of $\phi = 0.71$ and $\phi = 0.29$, respectively. The Gaussian contributions to the reduced stress (eq 20) are shown in Figures 3 and 4 as well. They

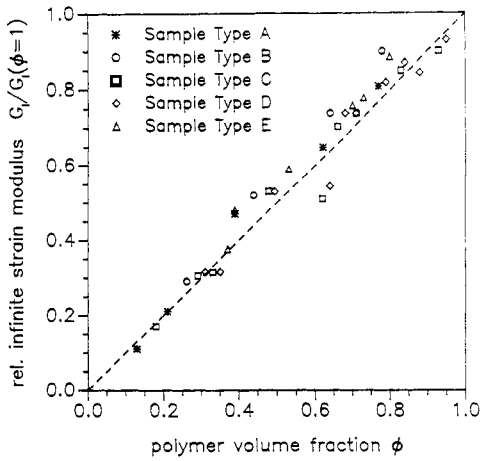

Figure 5. Plot of the ratio $G_I/G_I(\phi=1)$ against the polymer volume fraction ϕ. [(– – –), theoretical curve due to eqs 13 and 14].

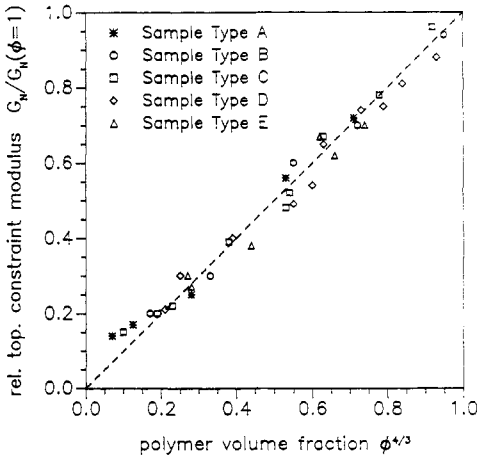

Figure 6. Plot of the ratio $G_N/G_N(\phi=1)$ against the polymer volume fraction $\phi^{4/3}$. [(– – –), theoretical curve due to eq 15].

are calculated in analogy to the unswollen samples according to eqs 21 and 22 by using the moduli and network parameters that are estimated for the samples of type C in the unswollen case (Table 2). The regression lines inserted in Figures 3 and 4 demonstrate the linear dependence of the Gaussian contributions to the reduced stress in these plots on a large extension scale. Its axis intersections at infinite strain are found to be almost independent of swelling degree as long as the same sample type is compared. According to the theoretical considerations in section 2.1, this means that the infinite strain modulus $G_c + G_eT_e$ changes linearly with ϕ. This is clearly shown in Figure 5, where the ratios between the infinite strain moduli of swollen and unswollen samples are plotted against the polymer volume fraction ϕ in swelling equilibrium. It is found that the expected proportionality in eqs 13 and 14 is fulfilled in good approximation.

The influence of swelling on the topological constraint modulus G_N is demonstrated by the different slopes of the regression lines in Figures 3 and 4. This follows from eq 20 and allows a test of the predicted proportionality (eq 15). Figure 6 shows a plot of the ratios between the topological constraint moduli for swollen and unswollen samples against $\phi^{4/3}$. It becomes obvious that eq 15 is fulfilled on a large scale of swelling degrees. The small deviations at small values of ϕ are probably related to the deswelling effect of the samples during the measurements. This already-discussed effect becomes more significant for highly swollen networks. In any case, there is no tendency of the topological constraint modulus to vanish at a finite polymer volume fraction ϕ. Especially, the plot

shown in Figure 4, which is found for a highly swollen sample, shows this clearly. The somehow mysterious critical value $\phi \approx 0.2$, where topological constraints are reported to vanish,[1,2,19] is not found if inverse Langevin statistics is applied for the distribution of network chains. Hence, this critical value is recognized to be an artifact of the insufficient Gaussian statistics only. The proposed $\phi^{4/3}$ dependence of topological constraints, which was already suggested by other authors,[35,36] is clearly confirmed by the presented experimental data. Deviations of the measured C_2 term from this behavior, which are reported in refs 3, 37, and 38, should be interpreted critically because the finite extensibility of chains is not considered in these papers. A final question of interest is the influence of the nature of the swelling diluent on stress–strain data that was found by Mark and co-workers.[3,37] In the present paper, no such influence of the diluents listed in Table 1 can be reported.

5. Conclusions

The consideration of finite extensibility of network chains together with topological chain constraints according to eqs 21 and 22 leads to some final results concerning the interpretation of the stress–strain properties of swollen rubber networks:

(A) The tubelike topological constraint modulus varies with polymer volume fraction according to the predictions of the tube model of Heinrich et al. ($G_N \sim \phi^{4/3}$). The swelling results of Figure 6 confirm the theoretically derived value $\nu = {}^1/_2$ for the exponent of the nonaffine tube deformation law (eq 1). In this sense, the present swelling results complete recent stress–strain experiments of unswollen networks,[13-15] together with NMR[15] and neutron scattering experiments.[16]

(B) The consideration of constraint release effects via an empirical parameter β, as assumed in ref 7, is not necessary for understanding the uniaxial stress–strain properties of swollen networks. Contrary to earlier results found in refs 1, 2, and 19, which were derived in the framework of Gaussian statistics, the topological constraint modulus G_N is found to vanish in the limit $\phi \to 0$, and not at a finite value $\phi \approx 0.2$.

(C) The structure factor A_c, which is related to the fluctuation of cross-links, is found to have the value $A_c = 0.67$, almost independent of the degree of swelling. This is concluded from the swelling dependence of the infinite strain modulus plotted in Figure 5.

(D) The segment number n that is estimated from stress–strain experiments of the unswollen samples can be used for the calculation of the Gaussian contribution to the reduced stress of the corresponding swollen samples as well. It means that a linear dependence of the Gaussian contribution to the reduced stress results in Mooney–Rivlin plots with the same number n for swollen and unswollen samples of the same type (Figures 3 and 4). This confirms the assumed swelling invariance of n (eq 22) and, hence, the applied network model.

References and Notes

(1) Gumbrell, S. M.; Mullins, L.; Rivlin, R. S. *Trans. Faraday Soc.* **1953**, *49*, 1495.
(2) Mullins, L. *J. Appl. Polym. Sci.* **1961**, *2*, 257; *Rubber Chem. Technol.* **1961**, *34*, 279.
(3) Mark, J. E. *Rubber Chem. Technol.* **1975**, *48*, 495.
(4) Kästner, S. *Faserforsch. Textiltech./Z. Polymerforsch.* **1976**, *27*, 1.
(5) Flory, P. J. *J. Chem. Phys.* **1977**, *66*, 5720.
(6) Ronca, G.; Allegra, G. *J. Chem. Phys.* **1975**, *63*, 4990.
(7) Heinrich, G.; Straube, E.; Helmis, G. *Adv. Polym. Sci.* **1988**, *85*, 33.
(8) Thomas, F.; Straube, E.; Helmis, G. *Plaste Kautsch.* **1975**, *22*, 411; **1978**, *25*, 577.
(9) Marrucci, G. *Macromolecules* **1981**, *14*, 434.
(10) Gaylord, R. J. *Polym. Eng. Sci.* **1979**, *19*, 263.
(11) Gaylord, R. J. *Polym. Bull.* **1982**, *8*, 325; **1983**, *9*, 186.
(12) Heinrich, G.; Straube, E. *Acta Polym.* **1983**, *34*, 589; **1984**, *35*, 115.
(13) Matzen, D.; Straube, E. *Colloid Polym. Sci.* **1992**, *270*, 1.
(14) Heinrich, G.; Vilgis, T. A. *Kautschuk + Gummi, Kunstst.* **1993**, *46*, 283.
(15) Gronski, W.; Hoffmann, W.; Simon, G.; Wutzler, A.; Straube, E. *Rubber Chem. Technol.* **1992**, *65*, 63.
(16) Straube, E.; Urban, V.; Richter, D.; Pyckhaut-Hintzen, W. *Macromolecules*, in press.
(17) Heinrich, G.; Straube, E. *Polym. Bull.* **1987**, *17*, 255.
(18) Morris, M. C. *J. Appl. Polym. Sci.* **1964**, *8*, 545.
(19) Treloar, L. R. G. *The Physics of Rubber Elasticity*, 3rd ed.; Clarendon Press: Oxford, 1975.
(20) Klüppel, M. *J. Appl. Polym. Sci.* **1993**, *48*, 1137.
(21) Klüppel, M. *Prog. Colloid Polym. Sci.* **1992**, *90*, 137.
(22) Klüppel, M. *Kautschuk + Gummi, Kunstst.* **1993**, *46*, 197.
(23) Edwards, S. F. *Phys. Soc.* **1967**, *92*, 9.
(24) Kästner, S. *Colloid Polym. Sci.* **1981**, *259*, 499, 508; *Polymer* **1979**, *20*, 1327; *Acta Polym.* **1980**, *31*, 444.
(25) Klüppel, M.; Heinrich, G. *Macromolecules* **1994**, *27*, 3596.
(26) Scanlan, J. *J. Polym. Sci.* **1960**, *43*, 501.
(27) Langley, N. R. *Macromolecules* **1968**, *1*, 348.
(28) Langley, N. R.; Polmanteer, K. E. *J. Polym. Sci., Polym. Phys. Ed.* **1974**, *12*, 1023.
(29) Heinrich, G.; Beckert, W. *Prog. Colloid Polym. Sci.* **1992**, *90*, 47.
(30) Edwards, S. F.; Vilgis, T. A. *Polymer* **1986**, *27*, 483; *Rep. Prog. Phys.* **1988**, *51*, 243.
(31) Kovac, J.; Crabb, C. C. *Macromolecules* **1982**, *15*, 537.
(32) Brandrup, J., Immergut, E. H., Eds. *Polymer Handbook*, 2nd ed.; Wiley-Interscience: New York, 1975.
(33) Aharoni, S. M. *Macromolecules* **1983**, *16*, 1722; **1986**, *19*, 426.
(34) Klüppel, M. *Kautschuk + Gummi, Kunstst.* **1994**, *47*, 242.
(35) Booth, C.; Gee, G.; Holden, G.; Williamson, R. M. *Polymer* **1964**, *5*, 343; *Rubber Chem. Technol.* **1965**, *38*, 314.
(36) van der Hoff, B. M. E. *Polymer* **1965**, *6*, 397.
(37) Yu, C. U.; Mark, J. E. *Macromolecules* **1974**, *7*, 229; *Rubber Chem. Technol.* **1974**, *47*, 1151.
(38) Flory, P. J.; Tatara, Y. *J. Polym. Sci., Polym. Phys. Ed.* **1975**, *13*, 683.